Study of the performances of low-cost adsorbents extracted from *Rosa damascena* in aqueous solutions decolorization

Majid Kermani[a,b], Hassan Izanloo[c], Roshanak Rezaei Kalantary[a,b],
Hossein Salehi Barzaki[d], Babak Kakavandi[e,f,*]

[a]*Research Center for Environmental Health Technology, Iran University of Medical Sciences, Tehran, Iran*
[b]*Department of Environmental Health Engineering, School of Public Health, Iran University of Medical Sciences, Tehran, Iran,
Tel. +98 21 86704627; emails: majidkermani@yahoo.com (M. Kermani), rezaei.r@iums.ac.ir (R.R. Kalantary)*
[c]*Research Center for Environmental Pollutants, Qom University of Medical Sciences, Qom, Iran
Tel. +98 25 37842227; email: h-izanloo@muq.ac.ir*
[d]*Department of Environmental Engineering, Islamic Azad University, West Tehran Branch, Tehran, Iran, Tel. +98 21 3458854;
email: salehi.h@yahoo.com*
[e]*Research Center for Health, Safety and Environment, Alborz University of Medical Sciences, Karaj, Iran*
[f]*Department of Environmental Health Engineering, Alborz University of Medical Sciences, Karaj, Iran, Tel. +98 26 34643398;
email: kakavandibvch@gmail.com*

ABSTRACT

Till date, few studies have been conducted in order to evaluate the efficiency of *Rosa Damascena* waste (RDW) for dyes removal from aqueous solution. In the present study, the powder and ash were prepared from RDW as inexpensive and locally-available materials for the preparation of the adsorbents to remove Reactive Red 198 (RR198) and Reactive Blue 29 (RB29) dyes from aqueous solution through batch experiments under operational factors namely, pH of solution, contact time, adsorbent dosage, initial dyes concentration and temperature. Physicochemical, morphological and structural properties of the adsorbents were also characterized using SEM and XRD instruments. Adsorption percentage of both dyes on the ash surfaces were significantly higher than that of powder. Results revealed that the adsorption efficiency increased with an enhancement in the adsorbent dosage and contact time. While, a decreasing trend was observed in dye adsorption with increasing the initial concentration of dyes. The equilibrium contact time was found to be 60 min for both the adsorbents. The experimental data were also best fitted with Langmuir isotherm and pseudo-second-order kinetic models. It was found that intraparticle diffusion was not the only rate-determining step of adsorption processes. The calculated values of the thermodynamic parameters such as $\Delta G°$, $\Delta H°$ and $\Delta S°$ demonstrated that the adsorption of RR198 and RB29 onto both the adsorbents were endothermic and spontaneous in nature. The adsorption percentage of RR198 and RB29 dyes on ash *Rosa Damascena* waste slightly declined from 88.8% to 61.0% and 91.3% to 66.1%, respectively, after five consecutive cycles. In conclusion, powder and ash derived from RDW are very effective and suitable adsorbents for reactive dyes removal from aquatic environment, due to their simple and cheap preparation, easy availability and good adsorption capacity.

Keywords: Low-cost adsorbent; *Rosa damascena*; Adsorption; Reactive dye; Modeling adsorption

* Corresponding author.

1. Introduction

The discharge of wastewater, containing dyes derived from plastics, textile and cosmetics industries, has recently been increased in volume. Dyes are widely used in industries for various purposes, for example, in chemistry laboratories for analytical purposes and in many biological and biomedical laboratories as biological stains [1]. The estimated annual production of dyes around the world is over 700,000 tons with 10,000 kinds of color, of which 10%–15% are discharged into the environment by the produced wastewaters [2]. It has been widely reported in the literature that industries mainly generate a strongly colored wastewater with a concentration in the range of 10–200 mg/L [3]. Dyes are organic compounds whose presence in the effluents increases the chemical oxygen demand and decreases their biological degradability [4]. Moreover, the presence of dyes in water resources can reduce the penetration of light into aqueous media and subsequent reduction of photosynthesis and dissolved oxygen, especially in the lower layers, thereby endangering the aquatic organism and microorganism's life [5,6]. Reactive dyes are known as the most widely used color substances in the textile industries, which have serious economic and environmental effects, due to their high solubility in water and spreading rapidly into the environment [7]. Therefore, with respect to the negative effects, structure and stability of these compounds, their complete removal from water and wastewater deems necessary [8].

Till date, several technologies have been applied for removing dyes from aqueous environments such as ion exchange [9], coagulation and flocculation [10], adsorption [11], advanced oxidation [12], membrane filtration [9,13] and biological [14] approaches. In addition, a large number of remediation methods such as membrane filtration, electrochemical degradation, irradiation and ozonation have been employed for dye removal. However, most of the above-mentioned remediation techniques are not only often expensive but also have operational limitations such as sludge production, hazardous by-products, and the problem of sludge disposal [15–18]. Because of their time-consuming fermentation processes and also inability to remove dyes, the biological methods are not regarded consistently as the effective and appropriate approaches. The chemical methods, such as coagulation and flocculation, are not suitable for removal of dyes with high solubility in water (e.g., reactive dyes) and often produce high volumes of sludge [5].

The adsorption is more popular than the other water purification approaches, due to its simplicity in operation, effectiveness, even at very low pollutant concentrations, and easy operation [19,20]. Furthermore, the production of high-quality effluents and the absence of hazardous substances such as ozone and free radicals are the other advantages of this process [11,21]. Recently, several adsorbents such as carbon nanotubes [22], zeolite [23], activated carbon (AC) [24] and bentonite [25] have been used to remove reactive dyes from aqueous media.

The application of AC in the adsorption process is more effective than the other materials which were used as adsorbents. With respect to its special physical, chemical and morphological features such as abundant surface area, porous structure and high adsorption capacity, AC has shown high potentials in dye removal [26]. However, the expensive restoration and production of AC have, to some extent, caused some serious restrictions against their application, so making it necessary to use low-cost adsorbents. The waste materials and the by-products of agriculture and industrial activities could be potentially used as low-cost adsorbents, due to their high availability and fewer processing requirements [27,28]. To date, many researchers have performed lots of studies to find novel, cheap and highly available adsorbents, and many authors are working to develop the application of cheap adsorbents. In this field, lots of research have been conducted to develop low-cost adsorbents [29,30]. In Iran, over 14,300 tons of Rosaceae are harvested annually which lead to obtaining 8,500 tons of *Rosa damascena* (RD). After distillation processes and extraction of essential oil, the wastes are discharged into environment without any use. Hence, it is an industrial waste which can be used as a potential source of an effective adsorbent.

To the best of our knowledge, no study has been conducted so far to evaluate the efficiency of *Rosa damascena* waste (RDW) for dyes removal from aqueous solutions. In addition, production of AC from RDW by physical activation method is not reported in the literature. On the other hand, very little work has been reported about reactive dyes adsorption on RDW. Hence, in the present work, the powder *Rosa damascena* waste (PRDW) and ash *Rosa damascena* waste (ARDW) were prepared from RDW as inexpensive and locally-available materials for the preparation of the adsorbents. The adsorbents were also characterized by using various techniques and their potentials were evaluated for the removal of Reactive Red 198 (RR198) and Reactive Blue 29 (RB29) dyes in a batch system separately. To model and describe the experimental equilibrium data of dyes removal, several equilibrium isotherm and kinetic models were used. The potential reusability of adsorbents was also examined.
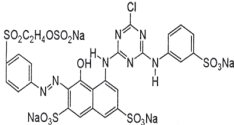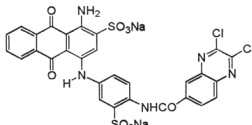
2. Materials and methods

2.1. Reagents and equipment

All chemicals were of analytical laboratory grade, purchased from Spectrum Chemical Co., Ltd., Shanghai, China, and used in all experiments without further purification. Two commercial textile dyes: Reactive Red 198 (RR198, 55% purity) and Reactive Blue 29 (RB29, ≥50% purity) were purchased from Alvan Sabet Co., Iran, and applied for preparation of stock solutions. The structure and some of the important physicochemical properties of the investigated dyes are given in Table 1. Deionized water (DI water) was used throughout all the experiments. A UV–visible spectrophotometer model CECIL-7100 was used to determine the residual dyes concentrations in the solution.

2.2. Adsorbent preparation and characterization

In this study, RDW was obtained from Kashan Province, center of Iran, which is available in abundance. For complete removal of impurities, the materials were initially washed several times with DI water. Then, the rinsed samples were dried at 100°C for 8 h. Afterwards, the samples were milled and eventually passed through a range of sieves to reach to the particle size between 250 and 300 μm diameter in

Table 1
Profile of RR198 and RB29 dyes used in the study

Characteristic	Dye	
	RR198	RB29
Chemical formula	$C_{27}H_{18}ClN_7Na_4O_{16}S_5$	$C_{29}H_{15}Cl_2N_5Na_2O_9S_2$
Commercial name	Reactive Red 198	Reactive Blue 29
Abbreviation	RR198	RB29
Class	Single azo class	Anthraquinone
C.I. number	18221	292775
Molecular weight (g/mol)	984.21	758.47
λ_{max} (nm)	518	596–600
Molecular structure		

accordance with the ASTM method [31]. The prepared powder was finally stored in plastic bags until use. In addition, Rosa ash was prepared through slow pyrolysis inside a furnace in an oxygen-free environment. In this method, a specific amount of powder was burned at 400°C temperature with heating rate of 25–35°C min⁻¹ for 2 h. Afterwards, the ash was washed with distillate water repeatedly to remove the dirt and dried at 100°C for 8 h. Then, it was passed through a 250–300 μm standard sieve. The adsorbent was again dried in an oven at 80°C–85°C for 2 h and finally stored in an air tight container for future use.

Table 2 represents the results of the analysis of the physicochemical characteristics of applied adsorbents (i.e., powder and ash). Also, for comparison, some of the physicochemical characteristics of commercial AC as an adsorbent of reference are presented. A CHNOS–Rapid elemental analytical instrument (Elementer, Germany) was used for the elemental analysis of both adsorbents. The bulk density and particle size distribution of adsorbents were also determined using Gay–Lussac pycnometer and sieve analysis, respectively. A digital microprocessor–based moisture analyzer (Mettler LP16) and ASTM D2866–11 was applied to determine the moisture and ash content of adsorbents, respectively. Furthermore, the specific surface area of PRDW and ARDW was measured by the Brunauer–Emmett–Teller (BET, Quantachrome, 2000, NOVA) using N₂ adsorption–desorption isotherms at 77.3 K. The pH zero point of charge (pH_pzc) of the adsorbents was determined, according to the procedure described by Cechinel et al. [32]. The surface morphologies of both adsorbents were obtained using a Philips XL-30 scanning electron microscope (SEM) (Philips Co., The Netherlands). The XRD patterns of PRDW and ARDW were obtained (X·Pert MPD, Philips, The Netherlands) using graphite monochromatic copper radiation (Cu Kα, λ = 1.54 Å) in the region of 10°–80° at 25°C.

2.3. Adsorption experiments procedure

The stock solutions of synthetic RR198 and RB29 with 500 mg/L concentration were prepared by dissolving their required amounts into the DI water. The effect of experimental

Table 2
Physicochemical characteristics of adsorbents used in this study

Parameters	Adsorbent		
	ARDW	PRDW	Commercial AC
Moisture content (%)	0.34	9.2	1.5–6
Volatile fraction (%)	0.19	10.9	0.1–1
Ash content (%)	0.06	17.89	2–10
Elemental analysis (%)			
C	54.9	77.8	93.2
H	2.3	2.1	0.2
N	3.1	2.56	0.1
O	39.7	17.22	6.5
S	ND	0.32	ND
pH_pzc	6.7	5.57	7.5–8
Bulk density (kg/m³)	315	230	150–440
BET surface area (m²/g)	35.8	13.3	600–1,500

variables such as the solution pH, the contact time, the adsorbent dosage, the initial dye concentration and the temperature on the adsorption efficiency was evaluated under batch-mode conditions. Batch experiments of dyes adsorption were conducted in 100 mL conical flasks containing 50 mL of solutions of dyes and varying adsorbent dosages. The samples were shaken at a constant rate of 300 rpm to reach adsorption equilibrium conditions. At appropriate time intervals, the aliquots were taken from the solutions and centrifuged at 5,000 rpm for 5 min to separate adsorbents particles. The residual dye concentrations in the solution were measured by a UV–visible spectrophotometer with the maximum absorption wavelengths of 518 nm for RR198 and 596 nm for RB29. All experiments were carried out in triplicate and the mean and the standard deviation (SD) of values were used to calculate the final results. The percentage of dyes removal ($R\%$) and the adsorption capacity, q_e (mg/g), were determined as follows:

$$q_e = (C_0 - C_e)(\frac{V}{M}) \tag{1}$$

$$\text{Removal (\%)} = (\frac{C_o - C_e}{C_o}) \times 100 \qquad (2)$$

where q_e is the adsorption capacity at equilibrium time (mg/g), V is the volume of the solution (L) and M is the dry weight of adsorbent (g). C_0 and C_e are the initial and residual dye concentrations (mg/L), respectively.

2.4. Adsorption optimization

To optimize the variables affecting RR198 and RB29 adsorption, the effects of the solution pH (in the range of 3.0–10.0) and contact time (at a period 3 h) were evaluated at initial dyes concentration of 25 mg/L in the presence of 4 g/L of adsorbent at room temperature (20°C ± 1°C). The initial pH of solution was adjusted by 0.1 M HCl and 0.1 M NaOH solutions. Afterwards, the impact of various dosages of powder and ash was evaluated over a range of 0.5–6 g/L. After optimization of factors, the adsorption kinetics and isotherms were investigated. Finally, thermodynamic studies were developed in the range of 20°C–50°C, under the optimized conditions.

3. Results and discussion

3.1. Adsorbent properties

The physicochemical characteristics of prepared adsorbents can be compared with commercial AC as an adsorbent of reference, as illustrated in Table 2. Accordingly, the values of surface area and bulk density of both prepared adsorbents were lower than that of AC, which might be associated with a difference in preparation and carbonization procedure as well as used materials. It is also notable that the amount of carbon (C) for PRDW and ARDW was lower than AC, indicating that the impurities of prepared adsorbents were mainly higher than commercial AC. For the other characteristics no significant difference was observed. The surface morphologies of PRDW and ARDW were analyzed using SEM (Philips, XL-30), at 15 keV. It can be seen that the ARDW surface is clearly different from that of the PRDW. As shown in Fig. 1, ARDW (Fig. 1(b)) has an irregular structure resulting in a rougher surface, while PRDW (Fig. 1(a)) has regular structure. Referring the SEM image, it seems that ARDW is more porous than PRDW and it can provide a noticeable adsorption capacity for pollutants removal.

The XRD pattern of the adsorbents was analyzed in the region of 10°–80° at 25°C. The XRD analysis results, shown in Fig. 2(a), revealed that the maximum peak (at 22°) was related to disordered and dispersed cristobalite which belongs to amorphous silica, according to the standard (JCPDS No. 29–0085) [33]. Thus, from the obtained results of XRD analysis, it can be concluded that silica is the major component in PRDW amorphous. There were no reflections likely associated with the crystalline phases of the other inorganic compounds present in PRDW. In the case of ARDW (Fig. 2(b)), however, two sharp peaks were observed at 26.5° and 29° in the pattern of ARDW, belonging to SiO_2 (JCPDS No. 85–0457) and $CaCO_3$ (JCPDS No. 86–2334), respectively. These results showed that silica in PRDW structure was oxidized to SiO_2 within ash preparation process from RDW.

3.2. Effect of contact time

The contact time between adsorbate and adsorbent is a critical experimental parameter affecting the performance of adsorption process. The effect of the contact time on the adsorption of RR198 and RB29 dyes by both adsorbents was evaluated during a 3 h time period and the results are shown in Fig. 3(a). The obtained results revealed that the removal efficiency of dyes increased rapidly during the initial steps of reaction and then kept an increasing trend at a relatively slow rate by increasing contact time and finally reached the equilibrium state after 60 min. The quick increase in the removal percentage in the initial stages can be ascribed to the existence of enormous vacant active sites in the adsorbent surface which were occupied by passing the contact time [5,34,35]. However, an increase in the contact time resulted in a decrease in the availability of dye molecules to active sites on the PRDW and ARDW surfaces that led to the reduction of the adsorption efficiency. Some studies have reported the same phenomenon in the investigation of reactive dyes adsorption on different adsorbents [36–38]. Hence, the contact time of 60 min was chosen as an equilibrium time of the
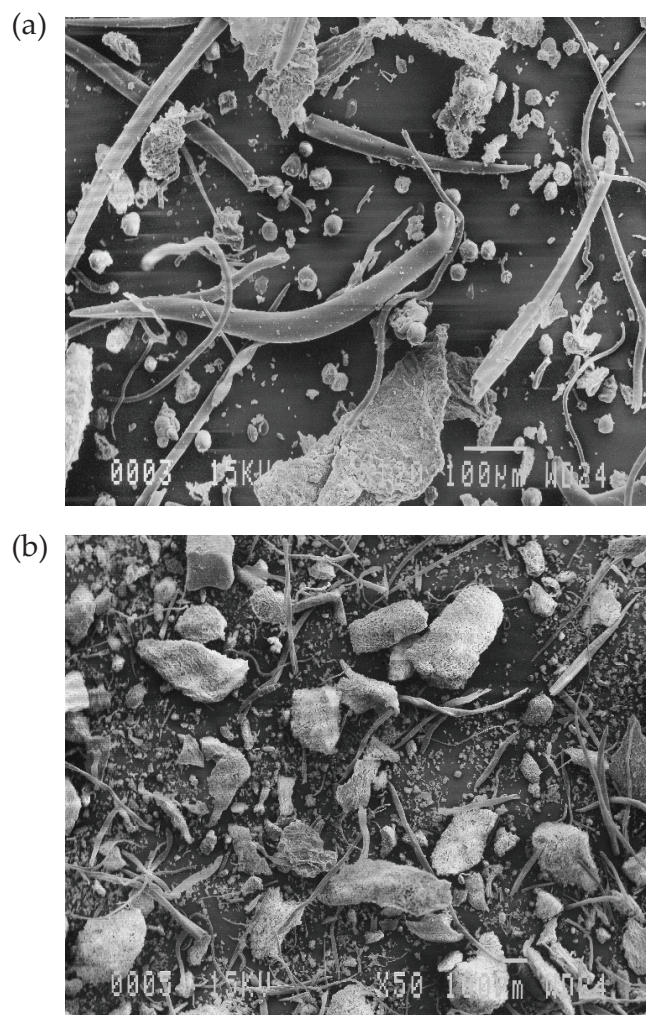
(a)

(b)

Fig. 1. Scanning electron microscope (SEM) images of PRDW (a) and ARDW (b) adsorbents.
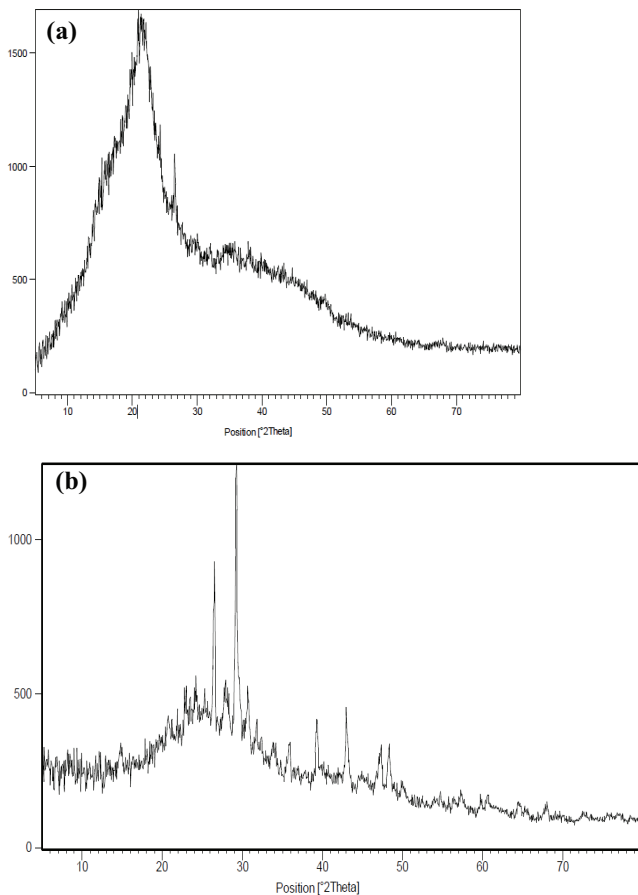
Fig. 2. X-ray diffraction of PRDW (a) and ARDW (b) adsorbents.

adsorption of RR198 and RB29 dyes onto PRDW and ARDW and used in the subsequent experiments.

3.3. Effect of pH

The initial solution pH is one of the most important parameters in adsorption process thereby affecting the adsorbent surface charges, the solution chemistry, and functional groups on the active sites [39]. Results of the effect of variation in the solution pH on the percentage of RR198 and RB29 dyes adsorption by PRDW and ARDW adsorbents at optimized contact time (60 min) are presented in Fig. 3(b). Accordingly, the rise in the pH of solution from 3 to 10 led to the falling of the removal dye percentages. As can be seen, the maximum adsorption efficiency of dyes was obtained at pH 3.0 for both adsorbents.

The high amount of dye adsorption at pH below 6.0–7.0 can be attributed to the electrostatic attraction between the adsorbent and the adsorbate molecules. Under these conditions, the surfaces of adsorbent have positive charges leading to an electrostatic attraction between RR198 and RB29 anionic dyes and adsorbents, which results in increasing the adsorption percentage. However, with increasing the solution pH, the electrostatic repulsion between the negatively charged molecules of dye and the negatively charged adsorbent surface reduced the dye adsorption [5,40,41]. In addition, at alkaline pH conditions, OH– ions exist in high
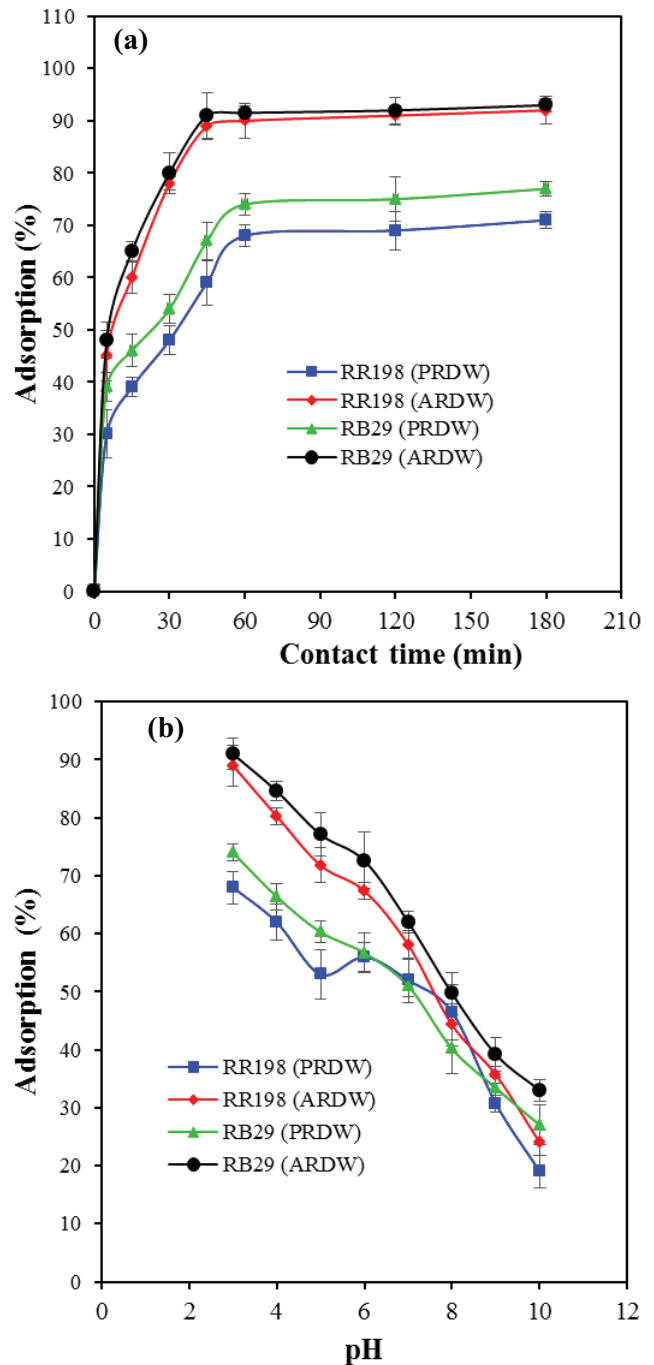

Fig. 3. Influence of contact time (a) and pH (b) on the RR198 and RB29 adsorption onto PRDW and ARDW adsorbents (experimental conditions: C_0 = 25 mg/L, adsorbent dosage = 4 g/L, 20 ± 1°C; a) pH = 4.0 and b) time = 60 min).

concentrations, which compete with RR198 and RB29 anionic dyes to occupy the active sites of the PRDW and ARDW surfaces [5]. Moreover, at acidic condition pH < pH_{pzc} (pH < 6.7 for ARDW and pH < 5.57 for PRDW), the surface is positively charged and thus, electrostatic attraction occurs between dye molecules and the adsorption sites, which tend to increase the adsorption percentages. However, at an equilibrium pH > pH_{pzc}, the surface of both adsorbents is negative and

subsequently the adsorption percentages of dyes dropped significantly, due to the electrostatic repulsion between negative surface charge and dyes molecule ions. With this background, as can be seen from Fig. 3(b), the adsorption efficiency of both dyes at acidic conditions (pH < 6.0–7.0) was higher than alkaline conditions. The optimum acidic pH has been observed for the reactive dyes adsorption on various adsorbents, as reported in the literatures [42,43]. Thus, pH 3.0 was chosen as an optimum solution pH for the future adsorption experiments.

3.4. Effect of different concentrations of adsorbent and adsorbate

The effect of various adsorbent and adsorbate concentrations on the adsorption efficiency and capacity was investigated in the range of 0.5–6 g/L and 25–300 mg/L, respectively, when the contact time was set at 60 min and pH was 3.0. It was found that the adsorption efficiency of RR198 and RB29 dyes under optimized conditions witnessed a significant drop with increasing the initial dye concentration from 25 to 300 mg/L. This is, probably, due to the fixed number of active sites on the adsorbent surfaces vs. increasing the number of dye molecules [44,45]. These findings are in good agreement with those of previous studies for several sorbent-reactive dyes sorption processes [5,46,47]. Referring to Fig. 4(b), it can be seen that the dyes uptake was increased by enhancing

Fig. 4. Influence of initial dye concentration (a) and adsorbent dose (b) on the RR198 and RB29 adsorption using PRDW and ARDW adsorbents (experimental conditions: time 60 min, pH = 3.0 and 20 ± 1°C; a) adsorbent dosage = 4 g/L and b) C_0 = 25 mg/L).

the adsorbents dosage from 0.5 to 6 g/L. While, it is observed from Fig. 4(b) that the sorption capacity of both dyes showed a significant drop with increasing the amount of adsorbents from 0.5 to 6 g/L. The most possible reason of an increase in the adsorption efficiency would be a rise in the adsorption surface rate, and consequently broad access of dye molecules to the adsorption sites on adsorbent [36,48]. However, the split in the flux or the concentration gradient between solute concentration in the solution and the solute concentration in the surface of the adsorbent could be a probable reason for the decrease in the adsorption capacity with increasing adsorbent dosage [49,50]. According to Fig. 4(b), the insignificant differences were observed in the removal efficiency of dyes when the adsorbents dosage increased from 4 to 6 g/L. So, the amount of 4 g/L was selected as an optimized dosage of the adsorbent for the adsorption process.

3.5. Adsorption modeling

3.5.1. Adsorption kinetic

The chemical kinetics are included in the investigations on how different experimental conditions can influence the speed of a chemical reaction. In the current study, three widely used kinetic models, including pseudo-first-order, pseudo-second-order and Weber–Morris intraparticle diffusion were employed to find the best-fitted model for the experimental data. The linear equations and the related values of kinetic parameters regarding RR198 and RB29 adsorption onto PRDW and ARDW are given in Table 3.

Results implied that both the adsorption processes follow pseudo-second-order model. The high values of the correlation coefficient (r^2) of the pseudo-second-order model, compared with the other models, suggest that pseudo-second-order model provides a better fitting to the experimental data. The plots of the adsorption kinetics (Fig. S1), also, confirm that the experimental data of dyes adsorption onto the studied adsorbents are in agreement with pseudo-second-order model. Moreover, a good agreement obtained when q_e had been calculated according to pseudo-second-order model, while the calculated amount of q_e derived from the pseudo-first-order model was not coherent with the experimental data. These observations demonstrate that both the adsorption processes can be better described by pseudo-second-order model, indicating that the concentrations of both adsorbent and adsorbate were the rate-controlling step of the adsorption processes of RR198 and RB29 dyes onto PRDW and ARDW [51].

3.5.2. Adsorption isotherm

Analysis of the equilibrium data is a critical point in designing adsorption systems [52]. Herein, Langmuir, Freundlich and Temkin models were applied to analyze the equilibrium data under the following experimental conditions: pH 3.0, adsorbent dose 4 g/L, initial concentration in the range of 25–300 mg/L and 20 ± 1°C. Langmuir and Freundlich isotherms are based on the homogeneous and the heterogeneous adsorption of adsorbate onto the adsorbent surfaces, respectively [48]. The empirical Freundlich model is based upon the assumption of multi-layer formation of adsorbate on the heterogeneous solid surface of the adsorbent and
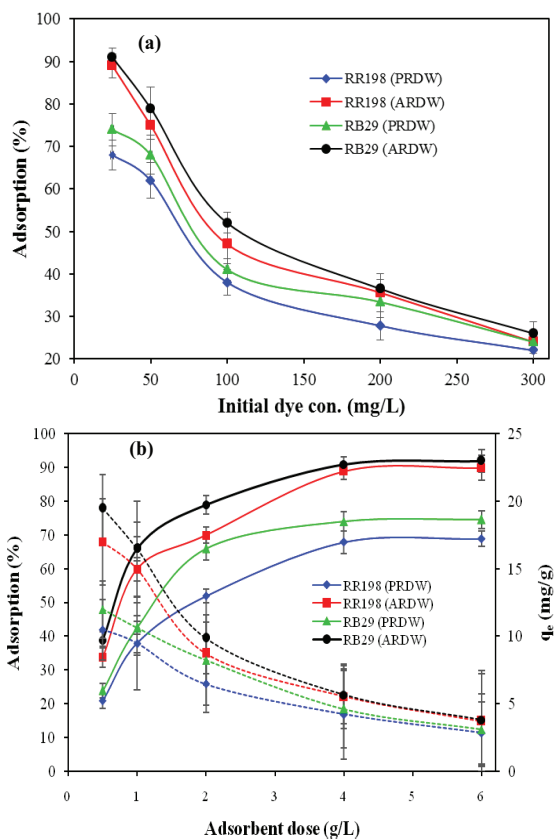
Table 3
Pseudo-first-order and pseudo-second-order parameters calculated from the adsorption kinetics of RR198 and RB29 on ARDW and PRDW (experimental conditions: C_0 = 25 mg/L, adsorbent dosage = 4 g/L, pH = 3.0 and T = 20 ± 1°C).

Adsorbent		Pseudo-first-order			Pseudo-second-order			$q_{e,exp}$
		Eq: $\ln(q_e - q_t) = \ln q_e - k_f t$ Plot: $\ln(q_e - q_t)$ vs. t			Eq: $t/q_t = t/q_e + 1/k_s q_e^2$ Plot: t/q_t vs. t			
		$q_{e,Cal}$ (mg/g)	k_1 (min^{-1})	r^2	$q_{e,Cal}$ (mg/g)	k_2 (g/mg.min)	r^2	
ARDW	RR198	6.05	0.91	0.9361	5.86	0.03	0.9991	5.62
	RB29	6.52	0.1	0.9103	5.9	0.035	0.9993	5.72
PRDW	RR198	3.55	0.04	0.9103	4.53	0.019	0.9967	4.25
	RB29	3.68	0.045	0.9234	5.06	0.02	0.9973	4.62

assumes that the stronger binding sites are occupied first, and then the binding strength decreases with the rise in the degree of site occupation [5]. Temkin model considers the effects of some indirect adsorbate/adsorbent interactions on the adsorption isotherms. As a result of adsorbate/adsorbent interactions, the heat of adsorption of all molecules in the layer would decrease linearly with the coverage [53].

The fundamental properties of Langmuir isotherm can be explained in terms of dimensionless separation factor R_L, ($R_L = 1/(1 + K_L C_0)$). The $R_L > 1$ values indicate unfavorable adsorption and for R_L of 1 and 0, the adsorption is linear and irreversible, respectively [44,54].

Table 4 reports the equations of isotherm models and the related parameters applied for the study of RR198 and RB29 adsorption onto the surfaces of PRDW and ARDW. Based on the table, all three isotherm models provide good correlation coefficients, r^2, for the adsorption of RR198 and RB29 dyes. However, the values of r^2 were larger than 0.98 for Langmuir isotherm model, indicating that this model could best fit the data of dyes adsorption onto PRDW and ARDW. It suggests that the homogeneous functional sites are distributed uniformly onto the surfaces of both adsorbents. Therefore, the uptake of dyes preferably follows the monolayer adsorption process [39]. Freundlich and Temkin models did not provide the significant correlation coefficients for the studied adsorption processes. This finding was, also, verified by a good agreement between the equilibrium data for the RR198 and RB29 adsorption experiments and the Langmuir equilibrium isotherm, as shown in Fig. S2. Previous studies have, also, reported that Langmuir isotherm was the best model for fitting the experimental data of reactive dyes adsorption on the other adsorbents as well [5,41,55]. It is observed in Table 4 that the values of R_L were between 0 and 1 in the Langmuir model, confirming that RR198 and RB29 dyes have been desirably adsorbed on the PRDW and ARDW adsorbents [5]. Furthermore, the desirability of the adsorption processes has been confirmed by the Freundlich exponent (n), since its values were 1 < n < 10 for both adsorbents [51,56].

3.5.3. Comparison with the other adsorbents

Table 5 shows a comparison between the obtained adsorption capacities of the applied adsorbents in the present study with the other applied adsorbents for the adsorptive removal of reactive dyes in the other research. The maximum amounts of RR198 and RB29 uptake per unit mass of adsorbent were 19.23 and 20.45 mg/g for ARDW and 18.2 and 19.9 for PRDW, respectively, based on Langmuir equilibrium model. It can be concluded that PRDW and ARDW have good maximum adsorption capacities in comparison with the other adsorbents. Therefore, they can be used as effective and promising adsorbents to remove organic dyes.

3.6. Mechanism of RR198 and RB29 adsorption

Generally, the process of adsorption of adsorbate onto the adsorbent surfaces occurs through multi-step mechanism involving: (a) outer (external) film diffusion, (b) intraparticle mass transfer and (c) adsorbate sorption on active site (chemical sorption) [63,64]. Since, the external film diffusion is resulted from the agitation of solution, the rate limiting step seems to be intraparticle diffusion and/or sorption on the active sites [63]. To deepen the understanding of this issue, we examined it, in terms of the intraparticle diffusion model, according to the following equation:

$$q_t = k_{id} t^{0.5} + C_i \tag{3}$$

where, q_t (mg/g) is the adsorption capacity at time t, k_{id} (mg/g min$^{0.5}$) is the constant rate of intraparticle diffusion, and C_i (mg/g) is relative to the thickness of the boundary layer. The k_{id} value can be determined by the slope of the linear plot of q_t vs. $t^{0.5}$ (Fig. 5), which is directly related to the adsorption rate controlled by intraparticle diffusion. Having a closer look to Table 6, the values of regression coefficient for intraparticle diffusion model was lower than 0.83, demonstrating that the intraparticle diffusion was not the only rate-determining step [11]. Moreover, C_i values of both dyes were not equal to zero, suggesting that the effect of the other mechanisms (i.e., chemical sorption or external mass transfer) had not been limited on the adsorption rate. These results also are confirmed by plots presented in Fig. 5, there curves did not pass through the origin [65]. Based on these results, it can be concluded that these two adsorbents have similar adsorption behaviors onto PRDW and ARDW.

3.7. Adsorption thermodynamic study

The thermodynamics of reactive dyes adsorption onto the adsorbents was investigated aiming to provide a deeper understanding of the process [39]. Herein, three

Table 4
Langmuir, Freundlich and Temkin parameters calculated from the adsorption isotherms of RR198 and RB29 on ARDW and PRDW (experimental conditions: C_0 = 25–300 mg/L, adsorbent dosage = 4 g/L, pH = 3.0, time = 60 min and T = 20 ± 1°C)

Isotherm models	Adsorbent/adsorbate			
	ARDW		PRDW	
	RR198	RB29	RR198	RB29
Langmuir isotherm				
$C_e/q_e = C_e/q_0 + 1/k_L q_0$				
q_0 (mg/g)	19.23	20.45	18.2	19.9
K_L (L/mg)	0.063	0.07	0.03	0.016
R^2	0.9887	0.9922	0.9871	0.9912
R_L	0.06–0.43	0.063–0.45	0.057–0.42	0.062–0.44
Freundlich isotherm				
$\ln q_e = \ln k_F + n^{-1} \ln C_e$				
k_F (mg/g(L/mg))$^{1/n}$	4.3	4.82	2.2	2.61
n	3.71	3.76	2.66	2.7
R^2	0.9734	0.9845	0.9648	0.9617
Temkin isotherm				
$q_e = B_1 \ln K_T + B_1 \ln C_e$				
K_T	2.04	2.51	2.33	1.92
B_1	2.92	3.03	3.44	3.75
R^2	0.9457	0.9783	0.9837	0.9783

main parameters, including changes in free energy ($\Delta G°$), enthalpy ($\Delta H°$) and entropy ($\Delta S°$), were determined to study the adsorption thermodynamics. The relationship concerning the thermodynamic parameters ($\Delta G°$, $\Delta H°$ and $\Delta S°$) is expressed, according to Eq. 4:

$$\ln K_d = \frac{\Delta S^o}{R} - \frac{\Delta H^o}{RT} \qquad (4)$$

where, K_d (q_e/C_e) is the distribution coefficient, q_e is the amount of dye adsorbed at equilibrium (mg/g) and C_e is the equilibrium concentration of dye in the solution (mg/L); R is the universal gas constant (8.314 J/mol K) and T is the absolute temperature (K). The values of $\Delta H°$ and $\Delta S°$ can be calculated from the slope and intercept of Vant Hoff plots of $\ln K_d$ vs. $1/T$ (Fig. 6), respectively.

The standard free energy ($\Delta G°$) can be calculated via Eq. (5):

$$\Delta G^o = -RT \ln K_d \qquad (5)$$

The influence of temperature (in the range of 20°C–50°C) on the dye adsorption and their thermodynamic behavior of adsorption were investigated under optimum conditions. Results showed that when solution temperature increased from 20°C to 50°C, the adsorption percentages of dyes on both the adsorbents showed an enhancing trend. This phenomenon can be explained by increasing the mobility of dye followed by an increase in the effective interactions between the adsorbate molecules and adsorbent surfaces. This finding suggests that RR198 and RB29 adsorption onto the adsorbents may be a kinetically controlled process. The calculated values of the thermodynamic parameters are presented in Table 7. The negative values of $\Delta G°$ suggest that the studied adsorption processes were feasible and had a spontaneous nature [44]. The negative values of $\Delta G°$ have increased as a result of increasing temperature, illuminating that the adsorption of RR198 and RB29 onto PRDW and ARDW are more favorable at higher temperatures [38,48]. As given in the Table 7, $\Delta H°$ has positive values, indicating that the adsorption process was endothermic and also suggesting that there should be a strong chemical bond between the dye molecules and the adsorbent surface [39,48]. The positive values of $\Delta S°$ suggest an increase in the degree of freedom by the adsorbed species [5,51].

3.8. Reusability of adsorbents

Reusability of adsorbent is a critical factor in terms of economic and resource recovery perspectives. The adsorbent regeneration and desorption of RR198 and RB29 dyes loaded on PRDW and ARDW were performed for five consecutive adsorption–desorption cycles. Initially, the performance of dyes adsorption was investigated with an initial dyes concentration of 25 mg/L under the optimized conditions (pH 3.0, contact time of 60 min, adsorbent dose of 4 g/L and temperature of 50°C) for five consecutive cycles. After the equilibrium time of the adsorption, the adsorbents were collected from the solutions and dried in an oven at 80°C for 60 min. Desorption experiments were, then, carried out using 0.1 M HCl as a desorbing solution. Hence, 0.1 g of PRDW and ARDW loaded with dyes were added to 10 mL of 0.1 M HCl solution and agitated for 12 h at 200 rpm and 25 ± 1°C.

Table 5
Comparison of RR198 and RB29 maximum adsorption capacity onto different adsorbents reported in literatures

| Adsorbent	Dye	Q_0	Kinetic	Isotherm	Ref
Alumina/carbon nanotube	Reactive Red 198	4.53	Pseudo-second-order	Langmuir	[57]
High lime fly ash	Reactive Black 5	7.18	pseudo-second-order	Freundlich	[58]
Potamogeton crispus	Reactive Red 198	44.2	Pseudo-second–order	Langmuir	[59]
PRDW	Reactive Red 198	18.2	Pseudo-second-order	Langmuir	This study
ARDW	Reactive Red 198	19.23	Pseudo-second-order	Langmuir	This study
Untreated alunite	Reactive Blue 114	2.92	Pseudo-second-order	Langmuir	[60]
Anodonta shell	Reactive green 12	0.436	pseudo-second-order	Langmuir and Freundlich	[61]
Untreated alunite	Reactive Red 124	2.85	Pseudo-second-order	Langmuir	[60]
Cotton stalk	Reactive Black 5	35.7	Pseudo–second-order	Langmuir	[62]
PRDW	Reactive Blue 29	19.9	Pseudo-second-order	Langmuir	This study
ARDW	Reactive Blue 29	20.45	Pseudo-second-order	Langmuir	This study
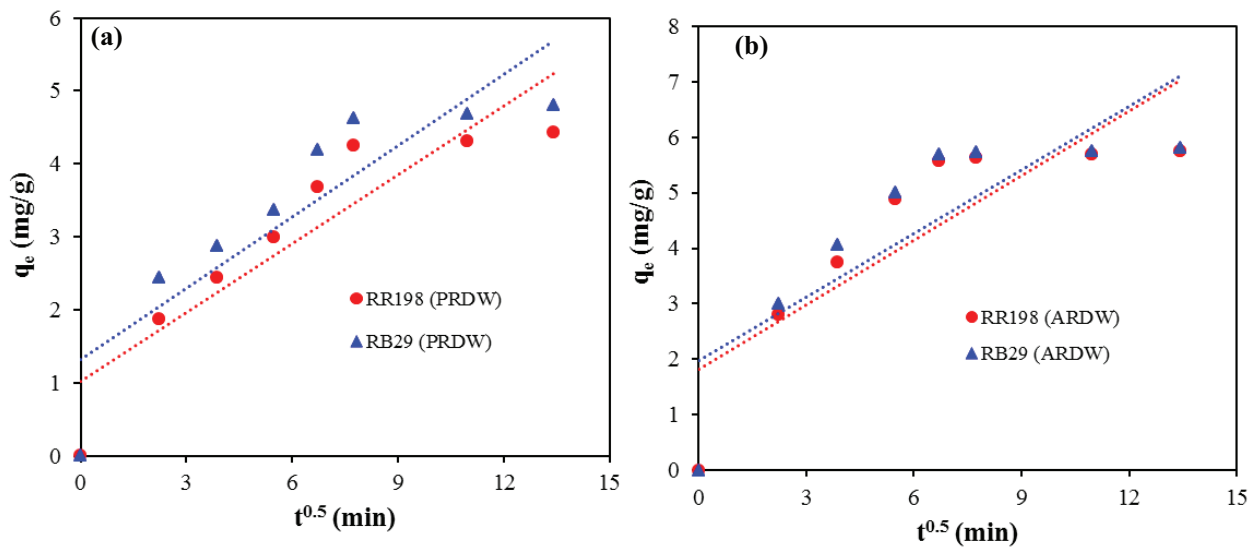
Fig. 5. Intraparticle diffusion plots for the adsorption of RR198 and RB29 on PRDW (a) and ARDW (b) at C_0 = 25 mg/L, adsorbent dosage = 4 g/L, pH = 3.0 and 20 ± 1°C.

Table 6
Intraparticle diffusion parameters calculated from the adsorption of RR198 and RB29 on ARDW and PRDW

Adsorbent	Dye	Intraparticle diffusion Eq: $q_t = k_{id}\, t^{0.5} + C_i$ Plot: q_t vs. $t^{0.5}$		
		k_{id}	C_i	R^2
PRDW	RR198	0.315	1.01	0.8307
	RB29	0.326	1.32	0.787
ARDW	RR198	0.387	1.81	0.718
	RB29	0.382	1.97	0.692

The desorption percentage (%DE) was calculated using the ratio of the amount of desorbed to the adsorbed dyes, as follows:

$$\%DE = \frac{\text{Desorbed dye (mg)}}{\text{Adsorbed dye (mg)}} \times 100 \qquad (6)$$
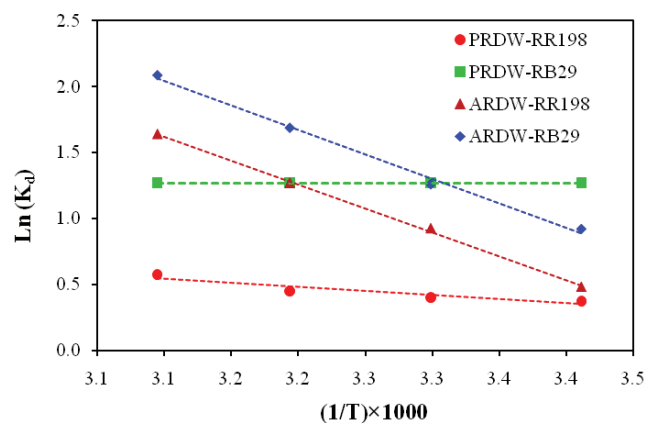

Fig. 6. Influence of temperature on the RR198 and RB29 adsorption by PRDW and ARDW adsorbents (experimental conditions: C_0 = 25 mg/L, time = 60 min, pH = 3.0 and adsorbent dosage = 4 g/L).

According to Fig. 7, no significant changes were observed in the reusability of adsorbents after five adsorption–desorption cycles. In the case of PRDW, the adsorption percentage of RR198 and RB29 dyes showed a slight decrease from 68.5% to 46.5% and 74.1% to 53.1%, respectively, after five cycles. Similar results were, also, observed for the adsorption of both dyes on ARDW when the application of ARDW slightly declined, the adsorption percentage of RR198 and RB29 dyes from 88.8% to 61.0% and 91.3% to 66.1%, respectively, after five cycles. These exhibit that both PRDW and ARDW adsorbents can be recycled and reused for a maximum of five successive cycles with an adsorption efficiency >46.0%. Additionally, it was observed that the desorption percentages of dyes from ARDW surface in the presence of HCl were higher than that from PRDW. The high desorption percentage may be due to the protonation of surface adsorbent with acidic agent. Hence, ARDW may be utilized as an economical and effective adsorbent for reactive dyes removal from aqueous solutions in industrial applications based on simple and easy regeneration.

Table 7
Thermodynamic parameters of RR198 and RB29 adsorption on the PRDW and ARDW

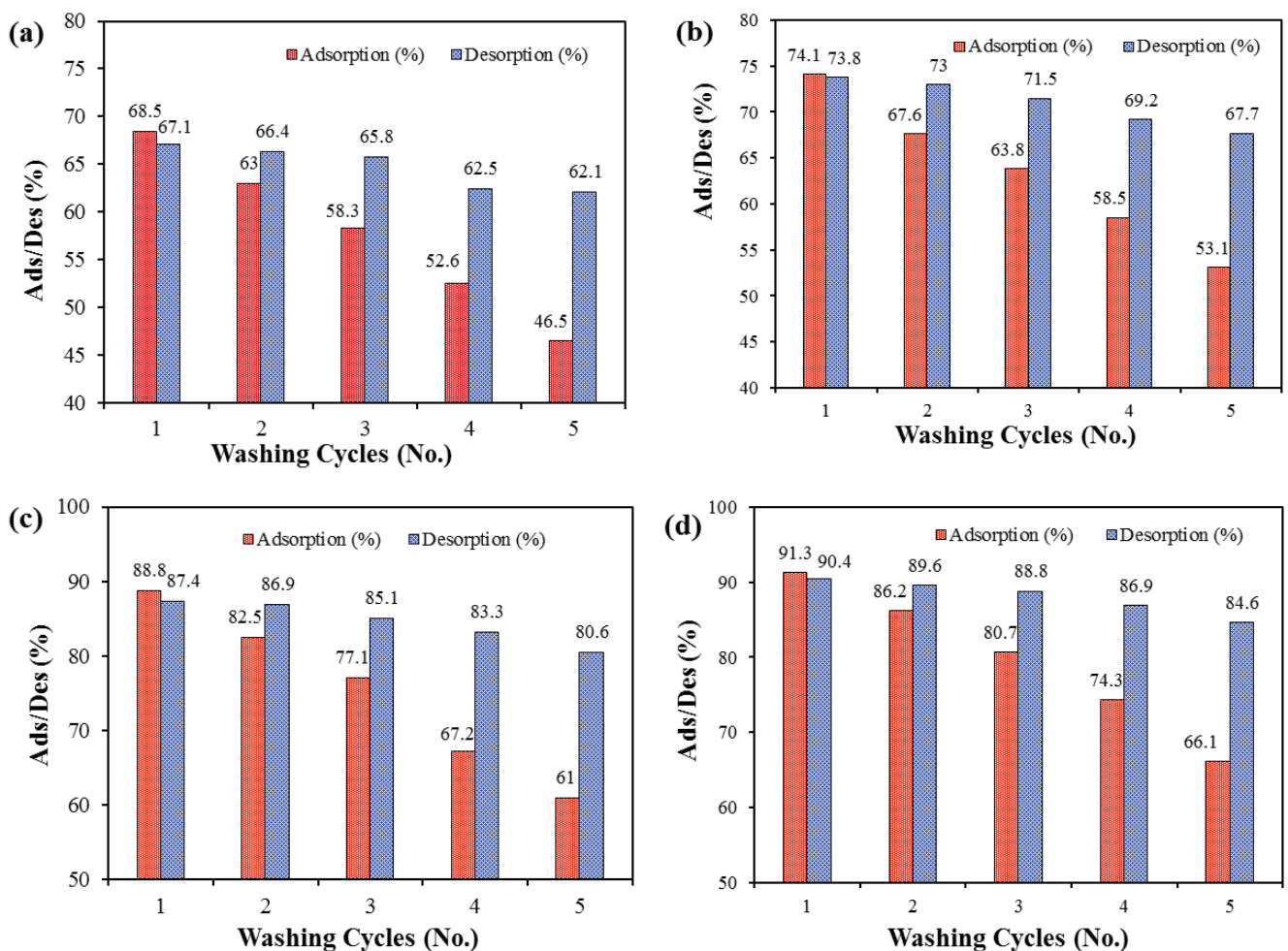| Adsorbent	Dye	$\Delta G°$ (kJ/mol)				$\Delta H°$ (kJ/mol)	$\Delta S°$ (kJ/mol K)
		$T = 20$	$T = 30$	$T = 40$	$T = 50$		
PRDW	RR198	−0.91	−1.01	−1.17	−1.54	7.54	0.021
	RB29	−3.09	−3.2	−3.3	−3.41	10.5	0.32
ARDW	RR198	−1.17	−2.33	−3.3	−4.4	24.9	0.09
	RB29	−2.25	−3.18	−4.4	−5.61	30.96	0.113

Fig. 7. Adsorption/desorption cycles of RR198 (a) and RB29 (b) by applying PRDW. Also, adsorption/desorption cycles of RR198 (c) and RB29 (d) by applying ARDW (experimental conditions: C_0 = 25 mg/L, time = 60 min, pH = 3.0 and adsorbent dosage = 4 g/L and 50 ± 1°C).

4. Conclusion

In this paper, the powder and ash derived from RDW were used as two low-cost adsorbents for the removal of RR198 and RB29 dyes from aqueous solution. The obtained results of the adsorption experiments exhibited that the removal of dyes is a pH-dependent process and the best removal efficiency was obtained at acidic conditions for both dyes. The kinetics of the adsorption process was found to follow the pseudo-second-order model. The equilibrium adsorption data of RR198 and RB29 on both adsorbents fitted better with the Langmuir isotherm model than the other isotherm models (i.e., Freundlich and Temkin), indicating that the adsorption of dyes onto PRDW and ARDW was a monolayer adsorption. Furthermore, results revealed that ARDW, compared with PRDW, provided better adsorption and desorption efficiency for both dyes. Thermodynamic studies showed that all the studied adsorption processes were feasible, spontaneous and endothermic in nature. In conclusion, PRDW and ARDW derived from RDW can be applied as effective adsorbents for reactive dyes removal from an aqueous solution, due to feasible and cost-effective production and excellent adsorption capacity.

References

[1] V.K. Gupta, R. Jain, A. Mittal, T.A. Saleh, A. Nayak, S. Agarwal, S. Sikarwar, Photo-catalytic degradation of toxic dye amaranth on TiO_2/UV in aqueous suspensions, Mater. Sci. Eng. C, 32 (2012) 12–17.

[2] X. Luo, Y. Zhan, Y. Huang, L. Yang, X. Tu, S. Luo, Removal of water-soluble acid dyes from water environment using a novel magnetic molecularly imprinted polymer, J. Hazard. Mater., 187 (2011) 274–282.

[3] G. Moussavi, M. Mahmoudi, Removal of azo and anthraquinone reactive dyes from industrial wastewaters using MgO nanoparticles, J. Hazard. Mater., 168 (2009) 806–812.

[4] V.K. Gupta, R. Kumar, A. Nayak, T.A. Saleh, M.A. Barakat, Adsorptive removal of dyes from aqueous solution onto carbon nanotubes: a review, Adv. Colloid Interface Sci., 193–194 (2013) 24–34.

[5] R. Rezaei Kalantry, A. Jonidi Jafari, A. Esrafili, B. Kakavandi, A. Gholizadeh, A. Azari, Optimization and evaluation of reactive dye adsorption on magnetic composite of activated carbon and iron oxide, Desal. Wat. Treat., 57 (2016) 6411–6422.

[6] Z. Rahmani, M. Kermani, M. Gholami, A.J. Jafari, N.M. Mahmoodi, Effectiveness of photochemical and sonochemical processes in degradation of Basic Violet 16 (BV16) dye from aqueous solutions, Iran. J. Environ. Health Sci. Eng., 9 (2012) 1–7.

[7] F. Nekouei, S. Nekouei, I. Tyagi, V.K. Gupta, Kinetic, thermodynamic and isotherm studies for acid blue 129 removal from liquids using copper oxide nanoparticle-modified activated carbon as a novel adsorbent, J. Mol. Liq., 201 (2015) 124–133.

[8] A. Safavi, S. Momenia, Highly efficient degradation of azo dyes by palladium/hydroxyapatite/Fe_3O_4 nanocatalyst, J. Hazard. Mater., 201–202 (2011) 125–131.

[9] J.-S. Wu, C.-H. Liu, K.H. Chu, S.-Y. Suen, Removal of cationic dye methyl violet 2B from water by cation exchange membranes, J. Membr. Sci., 309 (2008) 239–245.

[10] H. Issa Hamoud, G. Finqueneisel, B. Azambre, Removal of binary dyes mixtures with opposite and similar charges by adsorption, coagulation/flocculation and catalytic oxidation in the presence of CeO_2/H_2O_2 Fenton-like system, J. Environ. Manage., 195 (2017) 195–207.

[11] A.J. Jafari, B. Kakavandi, R.R. Kalantary, H. Gharibi, A. Asadi, A. Azari, A.A. Babaei, A. Takdastan, Application of mesoporous magnetic carbon composite for reactive dyes removal: process optimization using response surface methodology, Korean J. Chem. Eng., 33 (2016) 2878–2890.

[12] N.M. Mahmoodi, Photocatalytic ozonation of dyes using copper ferrite nanoparticle prepared by co-precipitation method, Desalination, 279 (2011) 332–337.

[13] X. Zhu, Y. Zheng, Z. Chen, Q. Chen, B. Gao, S. Yu, Removal of reactive dye from textile effluent through submerged filtration using hollow fiber composite nanofiltration membrane, Desal. Wat. Treat., 51 (2013) 6101–6109.

[14] L.K. Archna, R. Siva Kiran, Biological methods of dye removal from textile effluents – a review, J. Biochem. Technol., 3 (2012) S177–S180.

[15] B. Hameed, M. El-Khaiary, Equilibrium, kinetics and mechanism of malachite green adsorption on activated carbon prepared from bamboo by K_2CO_3 activation and subsequent gasification with CO_2, J. Hazard. Mater., 157 (2008) 344–351.

[16] S. Qu, F. Huang, S. Yu, G. Chen, J. Kong, Magnetic removal of dyes from aqueous solution using multi-walled carbon nanotubes filled with Fe_2O_3 particles, J. Hazard. Mater., 160 (2008) 643–647.

[17] A. Azari, A.-A. Babaie, R. Rezaei-Kalantary, A. Esrafili, M. Moazzen, B. Kakavandi, Nitrate removal from aqueous solution by carbon nanotubes magnetized with nano zero-valent iron, J. Mazandaran Univ. Med. Sci., 23 (2014) 15–27.

[18] A. Jonidi Jafari, B. Kakavandi, N. Jaafarzadeh, R. Rezaei Kalantary, M. Ahmadi, A. Akbar Babaei, Fenton-like catalytic oxidation of tetracycline by AC@Fe_3O_4 as a heterogeneous persulfate activator: adsorption and degradation studies, J. Ind. Eng. Chem., 45 (2017) 323–333.

[19] B. Kakavandi, M. Jahangiri-rad, M. Rafiee, A.R. Esfahani, A.A. Babaei, Development of response surface methodology for optimization of phenol and p-chlorophenol adsorption on magnetic recoverable carbon, Microporous Mesoporous Mater., 231 (2016) 192–206.

[20] A.A. Babaei, A. Azari, R.R. Kalantary, B. Kakavandi, Enhanced removal of nitrate from water using nZVI@ MWCNTs composite: synthesis, kinetics and mechanism of reduction, Water Sci. Technol., 72 (2015) 1988–1999.

[21] M. Kermani, H. Pourmoghaddas, B. Bina, Z. Khazaei, Removal of phenol from aqueous solutions by rice husk ash and activated carbon, Pak. J. Biol. Sci., 9 (2006) 1905–1910.

[22] L.D.T. Prola, F.M. Machado, C.P. Bergmann, F.E. de Souza, C.R. Gally, E.C. Lima, M.A. Adebayo, S.L.P. Dias, T. Calvete, Adsorption of Direct Blue 53 dye from aqueous solutions by multi-walled carbon nanotubes and activated carbon, J. Environ. Manage., 130 (2013) 166–175.

[23] C. Li, H. Zhong, S. Wang, J. Xue, Z. Zhang, Removal of basic dye (methylene blue) from aqueous solution using zeolite synthesized from electrolytic manganese residue, J. Ind. Eng. Chem., 23 (2015) 344–352.

[24] A. Jonidi Jafari, R. Rezaei Kalantary, A.A. Babaei, M. Heydari Farsani, B. Kakavandi, Modeling and optimization of adsorption process of reactive dyes on powder activated carbon modified by magnetite nanocrystals, J. Mazandaran Univ. Med. Sci., 26 (2016) 171–187.

[25] T. Anirudhan, M. Ramachandran, Adsorptive removal of basic dyes from aqueous solutions by surfactant modified bentonite clay (organoclay): kinetic and competitive adsorption isotherm, Process Saf. Environ. Protect., 95 (2015) 215–225.

[26] K. Foo, B.H. Hameed, An overview of dye removal via activated carbon adsorption process, Desal. Wat. Treat., 19 (2010) 255–274.

[27] A.A. Babaei, S.N. Alavi, M. Akbarifar, K. Ahmadi, A. Ramazanpour Esfahani, B. Kakavandi, Experimental and modeling study on adsorption of cationic methylene blue dye onto mesoporous biochars prepared from agrowaste, Desal. Wat. Treat, 57 (2016) 27199–27212.

[28] B. Bina, M. Kermani, H. Movahedian, Z. Khazaei, Biosorption and recovery of copper and zinc from aqueous solutions by nonliving biomass of marine brown algae of *Sargassum* sp., 9 (2006) 1525–1530.

[29] M. Ghaedi, H. Hossainian, M. Montazerozohori, A. Shokrollahi, F. Shojaipour, M. Soylak, M.K. Purkait, A novel acorn based adsorbent for the removal of brilliant green, Desalination, 281 (2011) 226–233.

[30] A.W. Samsuri, F. Sadegh-Zadeh, B.J. Seh-Bardan, Adsorption of As(III) and As(V) by Fe coated biochars and biochars produced from empty fruit bunch and rice husk, J. Environ. Chem. Eng., 1 (2013) 981–988.

[31] American Society for Testing and Material (ASTM), Annual Book of ASTM, Standard Test Method for Performing the Sieve Analysis of Coal and Designating Coal Size, Method D4749, USA, 2012.

[32] M.A.P. Cechinel, S.M.A.G. Ulson de Souza, A.A. Ulson de Souza, Study of lead (II) adsorption onto activated carbon originating from cow bone, J. Cleaner Prod., 65 (2013) 342–349.

[33] X. Peng, F. Xu, W. Zhang, J. Wang, C. Zeng, M. Niu, E. Chmielewská, Magnetic Fe_3O_4@silica–xanthan gum composites for aqueous removal and recovery of Pb^{2+}, Colloids Surf., A, 443 (2014) 27–36.

[34] R.M. Cavalcanti, W.A.G. Pessoa Jr., V.S. Braga, I.d.C.L. Barros, Adsorption of sulfur compound utilizing rice husk ash modified with niobium, Appl. Surf. Sci., 355 (2015) 171–182.

[35] R.R. Kalantary, A.J. Jafari, B. Kakavandi, S. Nasseri, A. Ameri, A. Azari, Adsorption and magnetic separation of lead from synthetic wastewater using carbon/iron oxide nanoparticles composite, J. Mazandaran Univ. Med. Sci., 24 (2014) 172–183.

[36] A.H. Sulaymon, W.M. Abood, Equilibrium and kinetic study of the adsorption of reactive blue, red, and yellow dyes onto activated carbon and barley husk, Desal. Wat. Treat., 52 (2014) 5485–5493.

[37] D. Angın, T.E. Köse, U. Selengil, Production and characterization of activated carbon prepared from safflower seed cake biochar and its ability to absorb reactive dyestuff, Appl. Surf. Sci., 280 (2013) 705–710.

[38] A.A. Babaei, A. Khataee, E. Ahmadpour, M. Sheydaei, B. Kakavandi, Z. Alaee, Optimization of cationic dye adsorption on activated spent tea: equilibrium, kinetics, thermodynamic and artificial neural network modeling, Korean J. Chem. Eng., 33 (2015) 1352–1361.

[39] B. Kakavandi, R.R. Kalantary, A.J. Jafari, S. Nasseri, A. Ameri, A. Esrafili, A. Azari, Pb(II) adsorption onto a magnetic composite of activated carbon and superparamagnetic Fe_3O_4 nanoparticles: experimental and modeling study, CLEAN Soil Air Water, 43 (2015) 1157–1166.

[40] Y.S. Al-Degs, M.I. El-Barghouthi, A.H. El-Sheikh, G.M. Walker, Effect of solution pH, ionic strength, and temperature on adsorption behavior of reactive dyes on activated carbon, Dyes Pigm., 77 (2008) 16–23.

[41] H. Xiao, H. Peng, S. Deng, X. Yang, Y. Zhang, Y. Li, Preparation of activated carbon from edible fungi residue by microwave assisted K_2CO_3 activation—application in reactive black 5 adsorption from aqueous solution, Bioresour. Technol., 111 (2012) 127–133.

[42] M. Yazdanbakhsh, H. Tavakkoli, S.M. Hosseini, Characterization and evaluation catalytic efficiency of $La_{0.5}Ca_{0.5}NiO_3$ nanopowders in removal of reactive blue 5 from aqueous solution, Desalination, 281 (2011) 388–395.

[43] Y. Xue, H. Hou, S. Zhu, Adsorption removal of reactive dyes from aqueous solution by modified basic oxygen furnace slag: isotherm and kinetic study, Chem. Eng. J., 147 (2009) 272–279.

[44] B. Kakavandi, A. Jonidi Jafari, R. Rezaei Kalantary, S. Nasseri, A. Ameri, A. Esrafily, Synthesis and properties of Fe_3O_4-activated carbon magnetic nanoparticles for removal of aniline from aqueous solution: equilibrium, kinetic and thermodynamic studies, Iran. J. Environ. Health Sci. Eng., 10 (2013) 1–9.

[45] M. Farzadkia, M. Gholami, M. Kermani, K. Yaghmaeian, Biosorption of hexavalent chromium from aqueous solutions by chemically modified brown algae of *Sargassum* sp. and dried activated sludge, Asian J. Chem., 24 (2012) 5257–5263.

[46] M.Ş. Tanyildizi, Modeling of adsorption isotherms and kinetics of reactive dye from aqueous solution by peanut hull, Chem. Eng. J., 168 (2011) 1234–1240.

[47] M. Ghaedi, B. Sadeghian, A.A. Pebdani, R. Sahraei, A. Daneshfar, C. Duran, Kinetics, thermodynamics and equilibrium evaluation of direct yellow 12 removal by adsorption onto silver nanoparticles loaded activated carbon, Chem. Eng. J., 187 (2012) 133–141.

[48] B. Kakavandi, R. Rezaei Kalantary, M. Farzadkia, A.H. Mahvi, A. Esrafili, A. Azari, A.R. Yari, A.B. Javid, Enhanced chromium (VI) removal using activated carbon modified by zero valent iron and silver bimetallic nanoparticles, J. Environ. Health Sci. Eng., 12 (2014) 1–10.

[49] J. Lin, Y. Zhan, Adsorption of humic acid from aqueous solution onto unmodified and surfactant-modified chitosan/zeolite composites, Chem. Eng. J., 200 (2012) 202–213.

[50] A. Gholizadeh, M. Kermani, M. Gholami, M. Farzadkia, Kinetic and isotherm studies of adsorption and biosorption processes in the removal of phenolic compounds from aqueous solutions: comparative study, J. Environ. Health Sci. Eng., 1 (2013) 11–29.

[51] B. Kakavandi, A. Esrafili, A. Mohseni-Bandpi, A.J. Jafari, R.R. Kalantary, Magnetic Fe_3O_4@ C nanoparticles as adsorbents for removal of amoxicillin from aqueous solution, Water Sci. Technol., 69 (2014) 147–155.

[52] M. Massoudinejad, A. Asadi, M. Vosoughi, M. Gholami, B. Kakavandi, M. Karami, A comprehensive study (kinetic, thermodynamic and equilibrium) of arsenic (V) adsorption using $KMnO_4$ modified clinoptilolite, Korean J. Chem. Eng., 32 (2015) 2078–2086.

[53] A. Behnamfard, M.M. Salarirad, Equilibrium and kinetic studies on free cyanide adsorption from aqueous solution by activated carbon, J. Hazard. Mater., 170 (2009) 127–133.

[54] A. Gholizadeh, M. Kermani, M. Gholami, M. Farzadkia, K. Yaghmaeian, Removal efficiency, adsorption kinetics and isotherms of phenolic compounds from aqueous solution using rice bran ash, Asian J. Chem., 25 (2013) 3871–3878.

[55] S. Senthilkumaar, P. Kalaamani, K. Porkodi, P. Varadarajan, C. Subburaam, Adsorption of dissolved reactive red dye from aqueous phase onto activated carbon prepared from agricultural waste, Bioresour. Technol., 97 (2006) 1618–1625.

[56] A. Azari, B. Kakavandi, R.R. Kalantary, E. Ahmadi, M. Gholami, Z. Torkshavand, M. Azizi, Rapid and efficient magnetically removal of heavy metals by magnetite-activated carbon composite: a statistical design approach, J. Porous Mater., 22 (2015) 1083–1096.

[57] M. Malakootian, H.J. Mansoorian, A. Hosseini, N. Khanjani, Evaluating the efficacy of alumina/carbon nanotube hybrid adsorbents in removing Azo Reactive Red 198 and Blue 19 dyes from aqueous solutions, Process Saf. Environ. Protect., 96 (2015) 125–137.

[58] Z. Eren, F.N. Acar, Equilibrium and kinetic mechanism for Reactive Black 5 sorption onto high lime Soma fly ash, J. Hazard. Mater., 143 (2007) 226–232.

[59] O. Gulnaz, A. Sahmurova, S. Kama, Removal of Reactive Red 198 from aqueous solution by *Potamogeton crispus*, Chem. Eng. J., 174 (2011) 579–585.

[60] M. Özacar, I.A. Şengil, Adsorption of reactive dyes on calcined alunite from aqueous solutions, J. Hazard. Mater., 98 (2003) 211–224.

[61] S. Figueiredo, R. Boaventura, J. Loureiro, Color removal with natural adsorbents: modeling, simulation and experimental, Sep. Purif. Technol., 20 (2000) 129–141.

[62] Ö. Tunc, H. Tanacı, Z. Aksu, Potential use of cotton plant wastes for the removal of Remazol Black B reactive dye, J. Hazard. Mater., 163 (2009) 187–198.

[63] K.Z. Elwakeel, Removal of Reactive Black 5 from aqueous solutions using magnetic chitosan resins, J. Hazard. Mater., 167 (2009) 383–392.

[64] A.W. Ip, J.P. Barford, G. McKay, A comparative study on the kinetics and mechanisms of removal of Reactive Black 5 by adsorption onto activated carbons and bone char, Chem. Eng. J., 157 (2010) 434–442.

[65] M. Ahmadi, M. Foladivanda, N. Jaafarzadeh, Z. Ramezani, B. Ramavandi, S. Jorfi, B. Kakavandi, Synthesis of chitosan zero-valent iron nanoparticles-supported for cadmium removal: characterization, optimization and modeling approach, J. Water Supply Res. Technol. AQUA, 66 (2017) 116–130.
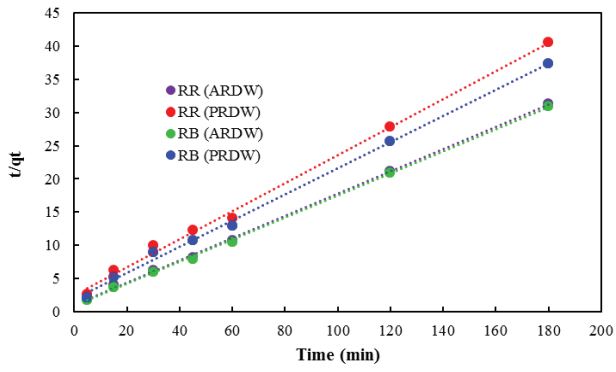
Supplementary material

Fig. S1. Pseudo-second-order plots of the adsorption of RR198 and RB29 onto PRDW and ARDW adsorbents.
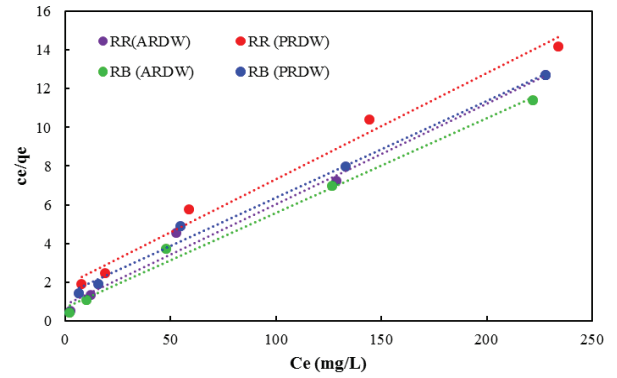

Fig. S2. Langmuir plots of the adsorption of RR198 and RB29 onto PRDW and ARDW adsorbents.